Smart Structures and Systems, *Vol. 36, No. 4 (2025) 203-211*
https://doi.org/10.12989/sss.2025.36.4.203

Rolling bearing fault diagnosis method based on WOA-VMD and CNN-SVM

Bo Liu*, Chunlei Zhang, Fuxiang Yu and Xiaofeng Wang

Dalian Scientific Test and Control Technology Institute, Dalian 116013, China

(*Received January 5, 2025, Revised August 6, 2025, Accepted September 2, 2025*)

Abstract. Aiming at the low accuracy of fault identification caused by insufficient fault feature extraction in vibration signals of rolling bearings, a fault diagnosis method based on whale algorithm to optimize variational modal decomposition parameters (WOA-VMD) for feature extraction and convolution neural network coupled with support vector machine (CNN-SVM) is proposed. Firstly, the parameters of VMD are optimized by WOA algorithm, and then some intrinsic modal components (IMF) are obtained by decomposing the fault signal by the VMD method. Then the IMF components are screened by correlation coefficient method, and the sample envelope entropy is further extracted as the feature vector. Finally, CNN-SVM classifier is used as a fault identification method to identify the faults of rolling bearings. The experimental results show that the WOA-VMD feature extraction method can accurately extract the fault information of rolling bearing vibration signals, and CNN-SVM classifier can effectively identify the fault features in bearing vibration signals. Compared with SVM and PSO-SVM classification methods, the proposed method can improve the fault recognition rate, and the accuracy rate can be improved to 99.6%.

Keywords: convolutional neural network; rolling bearing failure; sample envelope entropy; support vector machine; variational modal decomposition; whale optimization algorithm

1. Introduction

The fault of rolling bearing will seriously affect the safe and stable operation of rotating machinery and equipment, so the condition monitoring and fault diagnosis of rolling bearing has very important practical research significance, and many scholars have carried out various studies on it. Traditional methods use classical signal processing methods, such as Fast Fourier Transform (FFT) (Harvey 2014), Wavelet Transform (Benchabane *et al*. 2018, Prawin and Rao 2018), Empirical Mode Decomposition (EMD) (Zang *et al*. 2013, Liu and Lin 2012) and so on, to judge whether there is a fault in the characteristic frequency, but these methods have certain limitations and shortcomings, and lack of universality. In recent years, some new algorithms, such as Ensemble EMD (EEMD) (Wu and Huang 2009, Liu *et al*. 2017) and Variational Mode Decomposition (VMD) (Dragomiretskiy and Zosso 2014, Liu *et al*. 2022, Liu *et al*. 2025), have overcome some shortcomings of EMD algorithm and improved the efficiency of signal decomposition. At present, they have good application effects in bearing fault diagnosis. However, these methods still lack adaptive ability to decompose bearing vibration signals. For complex bearing fault signals, only relying on people's subjective parameter decomposition may lead to the omission of fault feature information and seriously affect the effect of fault diagnosis. For example, VMD algorithm is greatly influenced by setting parameters, and many scholars put forward corresponding optimization strategies for parameter setting (Chang *et al*. 2021, Liu *et al*. 2022, Liu *et al*. 2025). According to the number of affected modes of VMD algorithm results K and penalty factors α, the common way of parameter selection is to set parameters by human judgment (Sun *et al*. 2018), which lacks adaptability and affects the decomposition performance. In this paper, by analyzing the parameters K and α, in order to analyze the decomposition effect of VMD algorithm, a swarm intelligence algorithm— Whale optimization Algorithm (WOA) (Mirjalili and Lewis 2016, Amiri *et al*. 2020), which appeared in recent years, is proposed to optimize VMD parameters [K, α], VMD decomposition is carried out, and the minimum envelope entropy (Tang and Wang 2015) of each IMF component is calculated as the feature vector, thus improving the ability of fault feature extraction.

After fault feature extraction, it must be input into the pattern classifier for correct recognition, in order to make an effective diagnosis of fault patterns. At present, Support Vector Machines (SVM) (Cortes and Vapnik 1995, Chahnasir *et al*. 2018) is an effective nonlinear pattern recognition method for small samples. SVM is very dependent on the selection of parameters. Some scholars use the Particle Swarm Optimization (PSO) (Nguyen-Ngoc *et al*. 2021) to optimize SVM for fault diagnosis and identification (Liu *et al*. 2013), which improves the classification effect of SVM. In recent years, with the development of deep learning (Cui *et al*. 2024, Chen 2021, Lee *et al*. 2020), the application of convolutional neural networks (CNN) (Khan 2020, Park *et al*. 2020) to optimize the parameters of SVM can effectively improve the

*Corresponding author, Ph.D., Professor,
E-mail: liubo_1977@126.com; 31729134@qq.com

ISSN: 1738-1584 (Print), 1738-1991 (Online)

classification performance of SVM. Therefore, this paper adopts the fault diagnosis method of rolling bearing combined with CNN-SVM. CNN is used for feature extraction for initial identification, and then SVM classifier is used for further feature determination to accurately identify bearing faults. Compared with SVM classifier and PSO-SVM classifier, the classification accuracy of CNN-SVM has been effectively improved, which proves that the method combining WOA-VMD and CNN-SVM can extract fault features and diagnose performance more effectively.

2. The basic principle of VMD algorithm

The basic fame work of VMD algorithm is the construction and solution of variational problems. VMD algorithm redefines the decomposed IMF component, assuming the *k*th the expression of the IMF component is

$$u_k(t) = A_k(t)\cos\left(\phi_k(t)\right) \tag{1}$$

among them, $A_k(t)$ and $\phi_k(t)$ respectively are $u_k(t)$ instantaneous amplitude and instantaneous phase, and $\phi_k(t)$ is non-decreasing function, $\omega_k(t) = \dot{\phi_k}(t) \geq 0$ is the instantaneous angular frequency.

Perform the Hilbert transform on each IMF (Intrinsic Mode Function) component function $u_k(t)$, and get the unilateral spectrum of IMF component function

$$\left(\delta(t) + \frac{j}{\pi t}\right) * u_k(t) \tag{2}$$

$$\delta(t) = \begin{cases} 0 & t \neq 0 \\ \infty & t = 0 \end{cases}, \int_{-\infty}^{+\infty} \delta(t)dt = 1 \tag{3}$$

in the formula, δ(t) is Dirac function, the symbol "*" is a convolution operator.

The center frequency of each IMF component is estimated to $e^{-j\omega_k t}$ as a benchmark, frequency modulation of each IMF can be obtained.

$$\left[\left(\delta(t) + \frac{j}{\pi t}\right) * u_k(t)\right] e^{-j\omega_k t} \tag{4}$$

among them, ω_k is the center frequency, k is the number of IMF components.

After calculating the time derivative of the above formula, the sum of the signal bandwidths of each IMF component can be estimated by the square of the L^2 norm again, and the following optimization constrained variation problem can be constructed

$$\min_{\{u_k\},\{\omega_k\}} \left\{ \sum_k \left\| \partial_t \left[\left(\delta(t) + \frac{j}{\pi t}\right) * u_k(t) \right] e^{-j\omega_k t} \right\|_2^2 \right\} \tag{5}$$

$$s.t. \sum_{k=1}^{K} u_k = f \tag{6}$$

in the formula, K is the number of IMF components that need to be decomposed, $\{u_k\}$, $\{\omega_k\}$ correspond to the Kth IMF component and central frequency after decomposition, respectively. ∂_t is for finding partial derivative.

In order to solve the above-mentioned constrained variational problems, the Lagrange method should be used to transform the constrained problems into unconstrained ones.

$$L(\{u_k\},\{\omega_k\},\lambda) = \alpha \sum_{k=1}^{K} \left\| \partial_t \left[\left(\delta(t) + \frac{j}{\pi t}\right) \times u_k(t) \right] e^{-j\omega_k t} \right\|_2^2 + \left\| x(t) - \sum_{k=1}^{K} u_k(t) \right\|_2^2 + \left\langle \lambda(t), x(t) - \sum_{k=1}^{K} u_k(t) \right\rangle \tag{7}$$

among them, α represents the secondary penalty factor, λ(t) represents the Lagrange multiplication operator, $\langle\cdot\rangle$ represents the inner product operator.

For the solution of the above formula, the alternating direction multiplication method of multipliers (ADM) (Chen Qingguo 2018) is adopted, this algorithm iteratively updates $u_k(t)$, $\omega_k(t)$ and $\lambda(t)$ alternately to find the optimal solution of its saddle point, which is the constrained variational equation. The update and solution process of $u_k^{n+1}(t)$ is as follows

$$u_k^{n+1}(t) = argmin\left\{ \alpha \sum_{k=1}^{K} \left\| \partial_t \left[\left(\delta(t) + \frac{j}{\pi t}\right) \times u_k(t) \right] e^{-j\omega_k t} \right\|_2^2 + \left\| x(t) - \sum_{i \neq k}^{K} u_i(t) + \frac{\lambda(t)}{2} \right\|_2^2 \right\} \tag{8}$$

Using Fourier equidistant transformation, the above formula is transformed into frequency domain to solve, and the following results are obtained.

$$\hat{u}_k^{n+1}(\omega) = \frac{\hat{x}(\omega) - \sum_{i \neq k}^{K} \hat{u}_i(\omega) + \frac{\hat{\lambda}(\omega)}{2}}{1 + 2\alpha(\omega + \omega_k)^2} \tag{9}$$

where, the symbol "^" represents Fourier transform.

Similarly, the central frequency update solution is

$$\omega_k^{n+1} = \frac{\int_0^{\infty} \omega |\hat{u}_k(\omega)|^2 d\omega}{\int_0^{\infty} |\hat{u}_k(\omega)|^2 d\omega} \tag{10}$$

in the formula, ω_k^{n+1} represents the center of gravity of the current IMF component power spectrum.

The update formula of λ^{n+1} is

$$\lambda^{n+1} = \lambda^n + \tau\left(x - \sum_{k=1}^{K} u_k^{n+1} \right) \tag{11}$$

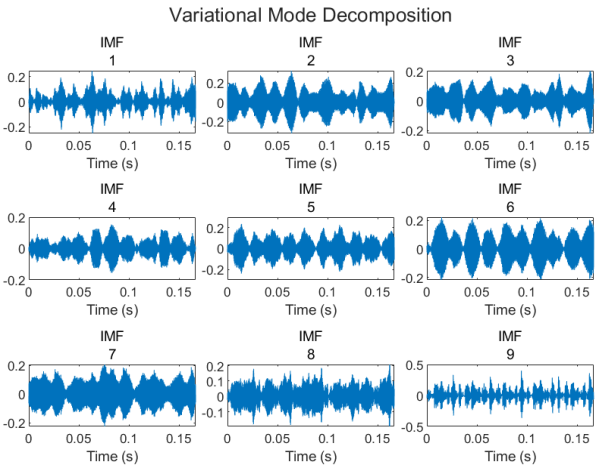

Fig. 1 Signal modal components

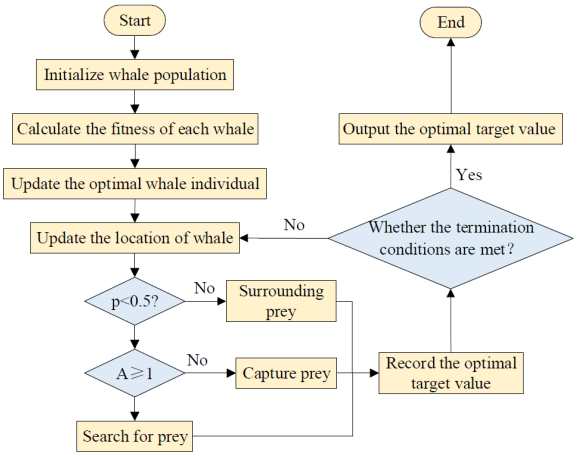

Fig. 2 Implementation process of WOA

in the formula, τ is the update factor.

Through the above analysis, the specific process of VMD algorithm is as follows:

① Initialize $\{u_k^1\}$, $\{\omega_k^1\}$, λ^1, and the value of n;

② $n = n + 1$, execute the loop program;

③ Update $\{u_k\}$, $\{\omega_k\}$;

④ $k = k + 1$, repeated updates $\{u_k\}$, $\{\omega_k\}$, until $k = K$;

⑤ Update λ^{n+1};

⑥ Set the discrimination accuracy ε, until the iteration stop condition is $\sum_k \|u_k^{n+1} - u_k^n\|_2^2 / \|u_k^n\|_2^2 < \varepsilon$ to end the loop. you can get K IMF component outputs.

For example, when the modal decomposition number is $K = 9$, $\alpha = 2500$, the decomposition result of VMD algorithm is shown in Fig. l.

3. Feature extraction of VMD parameters based on whale algorithm optimization (WOA-VMD)

According to the analysis in the previous section, the selection of two parameters K and α in VMD algorithm will affect its decomposition performance, but there is no definite pattern for the selection of K and α. Usually, a high K value can lead to excessive decomposition, while a low K value may result in insufficient signal decomposition; If the α value is too high, it will reduce the bandwidth of the decomposed IMF component, and if the α value is too low, it will increase the bandwidth of the IMF component. Therefore, selecting the appropriate values of parameters K and α is crucial for the effectiveness of VMD decomposition. Based on this, the WOA algorithm is used to optimize VMD parameters K and α, the minimum envelope entropy function is taken as the fitness function of WOA in this paper. Envelope entropy represents the sparsity of the original signal, when there is more noise and less feature information in the IMF component, the envelope entropy value is larger; On the contrary, the envelope entropy value is smaller (Tang and Wang 2015).

3.1 Whale optimization algorithm

Whale Optimization Algorithm (WOA) (Mirjalili and Lewis 2016, Amiri *et al*. 2020) is a swarm intelligence optimization algorithm based on biological inspiration, which is inspired by the bubble net predation behavior of humpback whales. The algorithm seeks the global optimal solution by simulating the whale predation process. Its basic principle includes three stages: surrounding prey, random search and spiral hunting. The specific implementation flow of WOA is as follows in in Fig. 2.

Among them, p is a random search probability, $p \in [0, 1]$; A is the convergence factor, A is a random value between $[-a, a]$, $a \in [0, 2]$.

3.2 WOA-VMD parameter optimization

The WOA algorithm is used to optimize the VMD parameters K and α. Firstly, the position of whale population is initialized, and the minimum value of envelope entropy (Zhao *et al*. 2022) is used as the fitness function. The envelope entropy E_p can be expressed as follows

$$E_p = -\sum_{i=1}^{N} \varepsilon(i) \, lg \, \varepsilon(i)$$
$$\varepsilon(i) = \frac{a(i)}{\sum_{i=1}^{N} a(i)} \tag{12}$$

in the formula, $a(i)$ is the decomposed envelope signal; $\varepsilon(i)$ is the normalized form of $a(i)$.

The steps of WOA-VMD parameter optimization algorithm are as follows:

① Initialize whale population position [K, α];

② The data signal is decomposed by VMD algorithm to obtain IMF components, and the envelope entropy of each IMF component is calculated;

③ The minimum envelope entropy function is used as the fitness function for global search;

④ Update the whale individual position according to

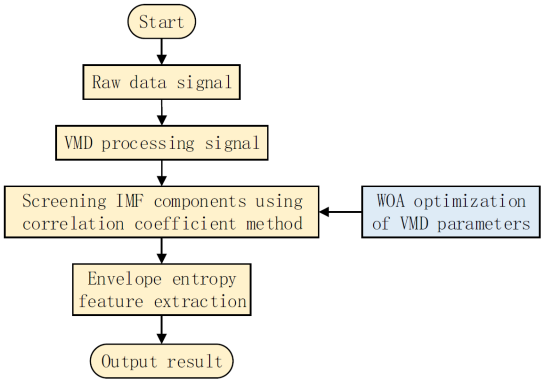

Fig. 3 Extraction process of feature vectors

the WOA main algorithm;

⑤ Judge the termination condition of the algorithm, so as long as the envelope entropy of the data signal reaches the minimum value or the set maximum number of iterations, the calculation can be stopped and the optimal parameter combination [K, α] can be output;

⑥ Set the control parameters of VMD algorithm with the optimal parameter combination, and perform variational modal decomposition on the data signal.

3.3 Extraction of feature vectors

After optimizing the parameters of VMD by WOA algorithm, the optimal parameter combination [K, α] of VMD decomposition is obtained. Using VMD algorithm to decompose the data signal, we can get K IMF components, calculate the correlation coefficient between each IMF component and the original data signal, and screen the IMF components according to the correlation coefficient, thus determining the IMF components to be extracted. The correlation coefficient is calculated according to the following formula

$$\rho[u_k(t)] = \left(x(t) - H\left(u_k(t)\right)\right) \otimes A_k(t) \tag{13}$$

in the formula, $\rho[u_k(t)]$ represents the correlation coefficient; $x(t)$ is an original data signal; $H\left(u_k(t)\right)$ is the power signal obtained by Hilbert transform of the kth IMF components; $A_k(t)$ is the amplitude of the kth IMF component; "⊗" represents convolution operation.

The number of screened IMF components is taken as the number of feature vectors, and the envelope entropy (Zhao *et al*. 2022) of each IMF component is calculated as the extracted feature vector. The extraction process of feature vectors is shown in Fig. 3.

4. Fault classification based on convolutional neural network and support vector machine

4.1 Convolutional Neural Network (CNN)

The basic structure of CNN includes: input layer, convolution layer, activation function, pooling layer, full connection layer and output layer, as shown in Fig. 4.

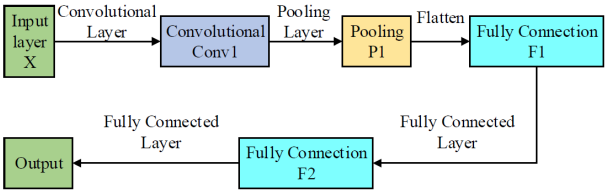

Fig. 4 CNN basic structure diagram

CNN calculation process is as follows:

(a) **Input layer**

Before inputting the data into the neural network, it is necessary to preprocess the data. The preprocessing method is to normalize the data, that is

$$y = \frac{x - x_{min}}{xmin_{max}} \tag{14}$$

in the formula, y represents the normalized data; x represents the original data; x_{max} represents the maximum value of the original data; x_{min} represents the minimum value of the original data.

(b) **Convolution layer**

The convolution layer uses convolution check to perform convolution operation on input data, and outputs a series of features through a nonlinear activation function. The calculation process is as follows

$$X^l = f(W^l \otimes X^{l-1} + B^l) \tag{15}$$

in the formula, X^l is the output of the lth layer; f(·) is a nonlinear activation function; W^l is the convolution kernel; X^{l-1} is the input quantity of the lth layer; B^l is the bias of the lth layer.

(c) **Pool layer**

Pool layer is to operate the input feature block to compress the data features to avoid over-fitting, and the calculation formula is

$$X^l = \phi(X^{l-1}) \tag{16}$$

in the formula, $\varphi(\cdot)$ is the pooling operator, this paper adopts the maximum pooling function.

(d) **Fully connected layer**

The fully connected layer is composed of multiple hidden layers, which is responsible for densely connecting each unit to all units in the previous layer. Specifically expressed as simple matrix multiplication plus offset, and then performing element-by-element nonlinear function activation, that is

$$X^l = f(W^l X^{l-1} + B^l) \tag{17}$$

(e) **Output layer**

The output layer is the classification layer, and CNN uses the softmax classifier for classification, and the calculation formula is

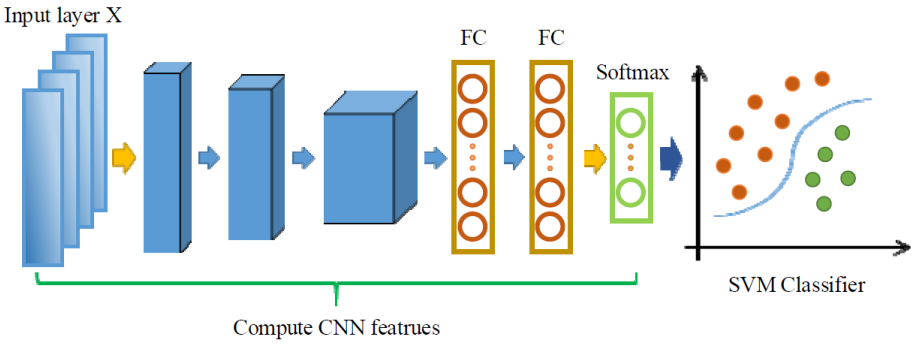

Fig. 5 The architecture of the proposed CNN-SVM

$$Y = g(X^{l-1}W^l + B^l) \tag{18}$$

in the formula, Y is the probability of outputting the corresponding input category; $g(\cdot)$ is the activation function of the output layer.

4.2 CNN-SVM fault classification

(a) Support Vector Machine (SVM)

SVM is a kind of generalized linear classifier for binary classification of data by supervised learning, and its decision boundary is the hyperplane of the maximum side distance for learning samples (Zhou 2016). For nonlinear problems, nonlinear SVM can be obtained by mapping input data into high dimensional space with nonlinear function and applying linear SVM. Nonlinear SVM has the following optimization problems

$$\min_{w,b}\left\{\frac{1}{2}\|w\|^2 + C\sum_{i=1}^{N}\xi_i\right\} \tag{19}$$

$$s.t. \quad y_i[w^T\varphi(X_i) + b] \geq 1 - \xi_i \quad \xi_i \geq 0 \quad i = 1,2,\cdots,N \tag{20}$$

in the formula, w is the normal vector of hyperplane; b is the deviation; C is a punishment factor; ξ_i is a relaxation variable. This formula is transformed into by Lagrange function and duality principle

$$\max_{\alpha}\left\{\sum_{i=1}^{N}\alpha_i - \frac{1}{2}\sum_{i=1}^{N}\sum_{j=1}^{N}[\alpha_i y_i \varphi(X_i)^T\varphi(X_j)y_j\alpha_j]\right\} \tag{21}$$

$$s.t. \quad \sum_{i=1}^{N}\alpha_i y_i = 0 \quad 0 \leq \alpha_i \leq C \quad i = 1,2,\cdots,N \tag{22}$$

in the formula, α_i is Lagrange multiplier; $\kappa(X_i, X_j) = \varphi(X_i)^T\varphi(X_j)$ is a kernel function. In this paper, RBF kernel function is used for classification.

When SVM algorithm deals with too many data features, it will reduce the diagnostic rate of the algorithm. As an intelligent optimization method, PSO algorithm has good local search ability. Using PSO algorithm to select the best parameter model of SVM can greatly improve the accuracy of fault diagnosis. However, the performance of PSO-SVM algorithm depends heavily on the selection of kernel and the setting of parameters, and it lacks adaptability. Moreover, the algorithm is usually shallow learning, and its ability to deal with large-scale data is weak, and the training process is time-consuming.

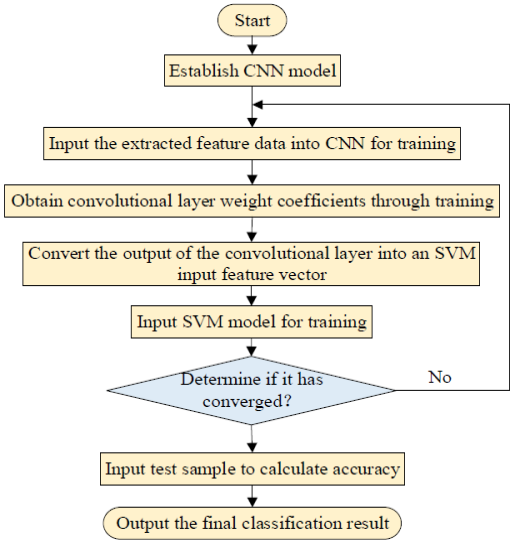

Fig. 6 Fault classification process of CNN-SVM

(b) CNN-SVM Classifier

In this paper, a CNN-SVM method is presented to learn a separable representation of vibriation signals in fault pattern recongnition of rolling bearings. The architecture of CNN-SVM is shown in Fig. 5.

The fault classification process of CNN-SVM is shown in Fig. 6.

5. Experimental results and analysis

5.1 Experimental data sources

The experimental data set is the bearing fault data set of Case Western Reserve University Bearing Data Center, the bearing to be detected supports the rotating shaft of the motor. The model of the driving end bearing is SKF6205, and the sampling frequency is 12 kHz. Set four kinds of test loads, and the corresponding rotating speeds are 1797 rpm,

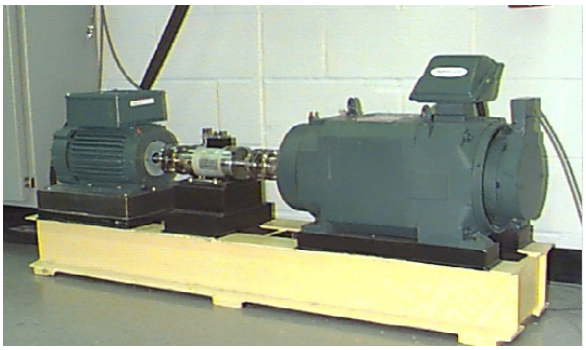

Fig. 7 Dynamic bearing fault simulation test bench

1772 rpm, 1750 rpm and 1730 rpm. Bearing damage is a single point damage by EDM, and the damage diameters are 0.1778 mm, 0.3556 mm and 0.5334 mm respectively. The bearing fault positions are rolling body fault, outer ring fault and inner ring fault respectively. Therefore, the fault state of bearing can be divided into 9 kinds and a normal bearing state. The following Fig. 7 shows a rolling bearing failure simulation test bench. In Fig. 7, the test bench includes a two-horsepower electric motor (left in the diagram), a torque sensor/demodulator (center in the diagram), a power tester (right in the diagram), and an electronic controller (not shown in the diagram).

The training data of the sample is bearing test speed of 1797 rpm and sampling frequency of 12 kHz. The sample contains 10 fault types in normal state, with 120 groups of data for each fault type and 2048 data points for each group. If the number of screened IMF components is 9, so there are a total of 1200 × 9 feature vectors. Specific fault types and labels are shown in Table 1.

5.2 Experimental model

The sample data set divides the input feature vector set into training set and test set according to the proportion of 80% and 20%, and then normalizes the data set according to Eq. (14). Aiming at the vibration signals of bearings in 10 States, the parameters of VMD are optimized by WOA algorithm, assuming the whale population size is 30, the maximum number of iterations is 20, the range of decomposition levels is [2, 10], and the range of penalty factors is [200, 4000], and then the best parameter combination [K, α] is found as shown in Table 2.

The optimized parameter VMD algorithm is used to decompose the bearing vibration signal, and the envelope entropy of the first nine IMF components is selected as the feature vector for sample training. The training samples of each fault state can be obtained 9×120 Envelope entropy. Selecting the minimum of 9 envelope entropy in each training sample as a set of feature vectors, 96 sets of

Table 1 Types and labels of faults

	Fault Type	Number of fault samples	Speed (rpm)	Label
NO. 1	Inner ring fault (IR007)	120	1797	1
NO. 2	Rolling element failure (B007)	120	1797	2
NO. 3	Outer ring fault (OR007)	120	1797	3
NO. 4	Inner ring fault (IR014)	120	1797	4
NO. 5	Rolling element failure (B014)	120	1797	5
NO. 6	Outer ring fault (OR014)	120	1797	6
NO. 7	Inner ring fault (IR021)	120	1797	7
NO. 8	Rolling element failure (B021)	120	1797	8
NO. 9	Outer ring fault (OR021)	120	1797	9
NO. 10	Normal state (N)	120	1797	10

Table 2 Best parameter combination [K, α]

	Fault type	Number of fault samples	Speed (rpm)	Label
NO. 1	Inner ring fault (IR007)	[10, 3325]	-7.43652	Inner ring fault (IR007)
NO. 2	Rolling element failure (B007)	[3, 803]	-7.33173	Rolling element failure (B007)
NO. 3	Outer ring fault (OR007)	[10, 2524]	-7.41345	Outer ring fault (OR007)
NO. 4	Inner ring fault (IR014)	[2, 203]	-7.14957	Inner ring fault (IR014)
NO. 5	Rolling element failure (B014)	[5, 477]	-7.00279	Rolling element failure (B014)
NO. 6	Outer ring fault (OR014)	[8, 2535]	-7.24607	Outer ring fault (OR014)
NO. 7	Inner ring fault (IR021)	[9, 2861]	-7.44073	Inner ring fault (IR021)
NO. 8	Rolling element failure (B021)	[8, 854]	-7.25085	Rolling element failure (B021)
NO. 9	Outer ring fault (OR021)	[7, 1870]	-7.42329	Outer ring fault (OR021)
NO. 10	Normal state (N)	[4, 930]	-6.81373	Normal state (N)

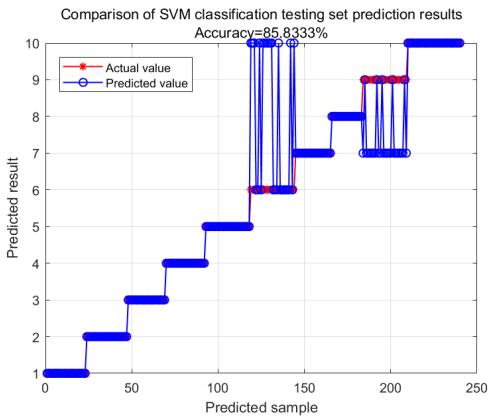

(a) Classification results

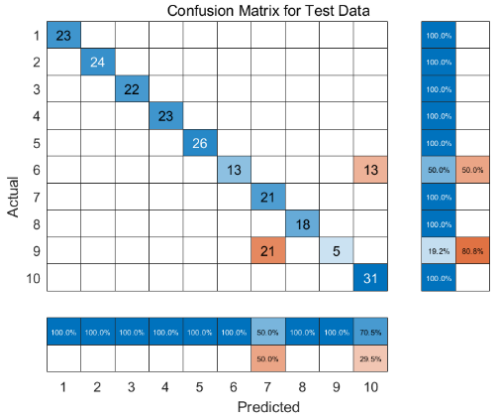

(b) Confusion matrix results

Fig. 8 Classification of SVM test samples

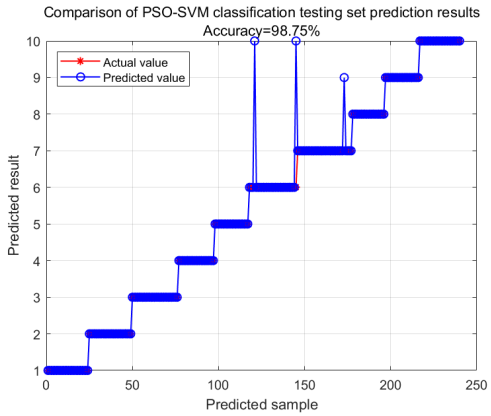

(a) Classification results

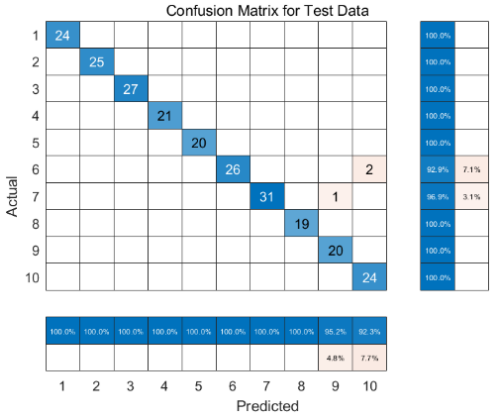

(b) Confusion matrix results

Fig. 9 Classification of PSO-SVM test samples

training set feature vectors and 24 sets of testing set feature vectors can be obtained. These eigenvectors are input into SVM classifier, PSO-SVM classifier and CNN-SVM classifier for training, and the prediction models in each fault state are obtained.

(a) Fault classification results by SVM classifier

The trained SVM classifier is used to classify the test-samples in 10 fault states, and the classification results and confusion matrix results of the test samples are shown in Fig. 8. The classification accuracy of test samples is 85.8333%; However, in the confusion matrix, diagonal elements represent the number of correct classifications. From the matrix diagram, it can be seen that fault numbers 6 and 9 are misclassified.

(b) The results of fault classification by PSO-SVM model

Similarly, WOA-VMD is used to extract the feature vectors of 10 kinds of bearing data, which are input into PSO-SVM model for fault identification, the population size of PSO is 50 and the maximum number of iterations is 100. The parameters of SVM are the same as those in SVM classifier in (a) Fault classification results by SVM classifier, that is, the optimization range of penalty factor C is [0.01,100] and the optimization range of radial basis function parameter G is [0.01,100]. There are 96 training sets and 24 testing sets in each fault state. The classification results of PS0-SVM model and the results of confusion matrix are shown in Fig. 9. The classification accuracy of test-samples is 98.75%, which is 12.9167% higher than that of SVM classifier. From the confusion matrix diagram, it can be seen that only a few samples in fault numbers 6 and 7 are wrongly classified.

(c) CNN-SVM model for fault classification results

The feature vectors of 10 kinds of bearing data extracted by WOA-VMD are transformed into two-dimensional images, and the input feature vector matrix is processed by numerical block through convolution layer and pool layer of CNN model, The CNN parameter is set to: the convolution kernel size is 3 × 10, the number is 32, and the size of the pool layer is 2 × 2. Based on the principle of maximum pooling, 80% of the data is randomly selected for training, and then the remaining 20% of the input-data is tested, the feature data after preliminary training is obtained through CNN activation layer as the input of SVM classifier, According to the fault classification process of CNN-SVM,

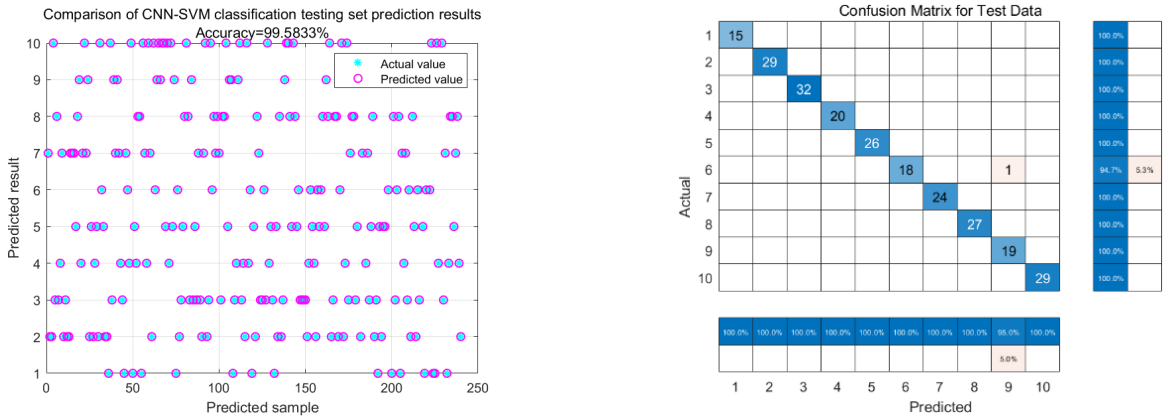

(a) Classification results (b) Confusion matrix results

Fig. 10 Classification of CNN-SVM test samples

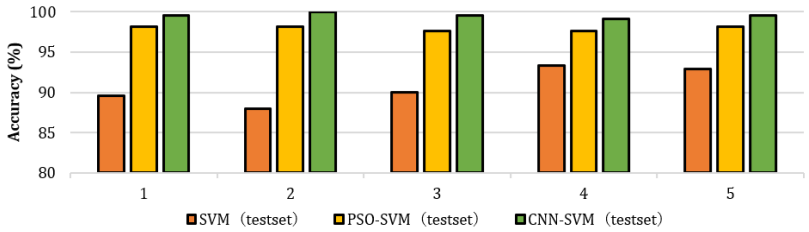

Fig. 11 Comparison of fault recognition accuracy with different experimental times

Table 3 Comparison of fault recognition accuracy between different algorithms

	Accuracy of fault identification		
	SVM	PSO-SVM	CNN-SVM
NO. 1	89.5833	98.1667	99.5833
NO. 2	87.9167	98.1667	100.0000
NO. 3	90.0000	97.5833	99.5833
NO. 4	93.3333	97.5833	99.1667
NO. 5	92.9167	98.1667	99.5833

SVM is used to judge whether the model converges, and the results of CNN-SVM classification and confusion matrix are shown in Fig. 10. The classification accuracy of test samples is 99.5833%, which is 13.75% and 0.8333% higher than that of SVM classifier and PSO-SVM classifier, respectively. From the confusion matrix diagram, it can be seen that only one sample in fault number 6 was wrongly classified.

To verify the validity of this model proposed in this article, five groups of comparative experiments were conducted. Compare the classification results of CNN-SVM algorithm proposed in this paper with those of SVM algorithm and PSO-SVM algorithm, as shown in Fig. 11. The fault identification accuracy of each group of experiments is shown in Table 3.

It can be concluded from the table that the average recognition rate of SVM algorithm is 90.75%, that of PSO-SVM algorithm is 97.9333%, and that of CNN-SVM algorithm is 99.5833%.

6. Conclusions

In this paper, a new method of rolling bearing fault diagnosis based on WOA-VMD feature extraction and CNN-SVM classifier is proposed. WOA algorithm is optimized to VMD algorithm to extract feature vectors, and then it is combined with CNN-SVM method for fault diagnosis. Firstly, the number of modes K and penalty parameters α in VMD is calculated by WOA for optimization, the bearing vibration signal is adaptively decomposed into a series of IMF components with fault characteristics, and the minimum envelope entropy of IMF is used as fitness function. The decomposed IMF is selected according to the correlation coefficient method, and the IMF components with strong correlation are further extracted and their sample envelope entropy is calculated as the feature vector to improve the separability of the vector. Secondly, CNN-SVM classifier is used as a fault recognition method to identify rolling bearings, and CNN model is used to learn from two-dimensional time series data, which improves the ability of feature extraction. On the basis of CNN's preliminary judgment of fault types, SVM method is used to effectively improve the accuracy of fault identification. Through comparative experiments, it is known that for the same diagnosis model, the accuracy of SVM, PSO-SVM and CNN-SVM are 90.75%, 97.9333% and 99.5833% respectively, which proves that the proposed fault recognition method has good generalization ability and higher recognition accuracy.

Acknowledgments

The research described in this paper was financially supported by the National Defense Basic Research Fund Project.

References

Amiri, G.G., Dehcheshmeh, M.M. and Hosseinzadeh, A.Z. (2020), "Feasibility study on model-based damage detection in shear frames using pseudo modal strain energy", *Smart Struct. Syst., Int. J.*, **25**(1), 47-56. https://doi.org/10.12989/sss.2020.25.1.047

Benchabane, F., Guettaf, A., Yahia, K. and Sahraoui, M. (2018), "Experimental investigation on induction motors inter-turns short-circuit and broken rotor bars faults diagnosis through the discrete wavelet transform", *e&i Elektrotechnik und Informationstechnik*, **135**, 187-194. https://doi.org/10.1007/s00502-018-0607-6

Chahnasir, E.S., Zandi, Y., Shariati, M., Dehghani, E., Toghroli, A., Mohamad, E.T., Shariati, A., Safa, M., Wakil, K. and Khorami, M. (2018), "Application of support vector machine with firefly algorithm for investigation of the factors affecting the shear strength of angle shear connectors", *Smart Struct. Syst., Int. J.*, **22**(4), 413-424. https://doi.org/10.12989/sss.2018.22.4.413

Chang, Y., Bao, G., Cheng, S., He, T. and Yang, Q. (2021), "Improved VMD-KFCM algorithm for the fault diagnosis of rolling bearing vibration signals", *IET Signal Process.*, **15**(4), 238-250. https://doi.org/10.1049/sil2.12026

Chen, Q.G. (2018), "A study on some problems of alternating direction method of multipliers", Masters Dissertation; China Jiliang University, Hangzhou, China.

Chen, W. (2021), *Computational Intelligence and Deep Learning*, XIDIAN University Press, Xi'an, SX, China.

Cortes, C. and Vapnik, V. (1995), "Support-vector networks", *Mach. Learn.*, **20**, 273-297. https://doi.org/10.1007/BF00994018

Cui, L., Wang, G., Liu, D., Xiang, J. and Wang, H. (2024), "Dual-loss CNN: A separability-enhanced network for current-based fault diagnosis of rolling bearings", *Smart Struct. Syst., Int. J.*, **33**(4), 253-262. https://doi.org/10.12989/sss.2024.33.4.253

Dragomiretskiy, K. and Zosso, D. (2014), "Variational mode decomposition", *IEEE Transact. Signal Process.*, **62**(3), 531-544. https://doi.org/10.1109/TSP.2013.2288675

Harvey, D. (2014), "Faster arithmetic for number-theoretic transforms", *J. Symbol. Computat.*, **60**(1), 113-119. https://doi.org/10.1016/j.jsc.2013.09.002

Khan, S. (2020), *A Guide to Convolutional Neural Networks for Computer Vision*, China Machine Press, Beijing, BJ, China.

Lee, S.J., Roh, M.I. and Oh, M.J. (2020), "Image-based ship detection using deep learning", *Ocean Syst. Eng., Int. J.*, **10**(4), 415-434. https://doi.org/10.12989/ose.2020.10.4.415

Liu, B. and Lin, Y. (2012), "A method for underwater image analysis using bi-dimensional empirical mode decomposition technique", *Ocean Syst. Eng., Int. J.*, **2**(2), 137-145. https://doi.org/10.12989/ose.2012.2.2.137

Liu, J., Liu, Z. and Xiong, Y. (2013), "Method of parameters optimization in SVM based on PSO", *Transact. Comput. Sci. Technol.*, Wuhan, China, March.

Liu, X., Liu, M. and Chen, Y. (2017), "Rolling bearing fault diagnosis based on EEMD-PE coupled with M-RVM", *J. Harbin Inst. Technol. Univ.*, **49**(9), 122-128. https://doi.org/10.11918/j.issn.0367-6234.201604066

Liu, J.L., Qiu, F.L., Lin, Z.P., Li, Y.Z. and Liao, F.Y. (2022), "A generalized adaptive variational mode decomposition method for nonstationary signals with mode overlapped components", *Smart Struct. Syst., Int. J.*, **30**(1), 75-88. https://doi.org/10.12989/sss.2022.30.1.075

Liu, J.L., Chen, R., Qiu, F.L., Yu, A.H., Zheng, W.T. and Wu, S.P. (2025), "Structural instantaneous frequency identification of non-stationary signals using GDAVMD and MSST", *Structures*, **72**, p. 108234. https://doi.org/10.1016/j.istruc.2025.108234

Mirjalili, S. and Lewis, A. (2016), "The whale optimization algorithm", *Adv. Eng. Software*, **95**, 51-67. https://doi.org/10.1016/j.advengsoft.2016.01.008

Nguyen-Ngoc, L., Tran, N.H., Bui-Tien, T., Mai-Duc, A., Abdel Wahab, M., X Nguyen, H. and De Roeck, G. (2021), "Damage detection in structures using particle swarm optimization combined with artificial neural network", *Smart Struct. Syst., Int. J.*, **28**(1), 1-12. https://doi.org/10.12989/sss.2021.28.1.001

Park, S., Jeong, H., Min, H., Lee, H. and Lee, S. (2020), "Wavelet-like convolutional neural network structure for time-series data classification", *Smart Struct. Syst., Int. J.*, **22**(2), 175-183. https://doi.org/10.12989/sss.2018.22.2.175

Prawin, J. and Rao, A. (2018), "Detection of nonlinear structural behavior using time-frequency and multivariate analysis", *Smart Struct. Syst., Int. J.*, **22**(6), 711-725. https://doi.org/10.12989/sss.2018.22.6.711

Sun, C., Wang, Y., Shen, Y. and Chen, W. (2018), "Fault diagnosis of planetary gearbox based on adaptive parameter variational mode decomposition", *J. Aerosp. Power*, **33**(11), 2756-2765. https://link.oversea.cnki.net/doi/10.13224/j.cnki.jasp.2018.11.022

Tang, G.J. and Wang, X.L., (2015), "Parameter optimized variational mode decomposition method with application to incipient fault diagnosis of rolling bearing", *J. Xi'an Jiaotong Univ.*, **49**(5), 73-81. https://doi.org/10.7652/xjtuxb201505012

Wu, Z. and Huang, N.E. (2009), "Ensemble empirical mode decomposition: A noise assisted data annlysis method", *Adv. Adapt. Data Anal.*, **1**(1), 1-41. https://doi.org/10.1142/S1793536909000047

Xu, J. (2019), "Research on fault diagnosis method of rolling bearing based on PSO-BP neural network and improved PSO-SVM", Masters Dissertation; Tianjin University, Tianjin, China.

Zhao, R.Z., Liu, Q. and Yang, Z.B. (2022), "Research of fault recognition method of rolling bearings based on K-VMD envelope entropy and SVM", *Noise Vib. Control*, **42**(3), 92-121. https://nvc.sjtu.edu.cn/EN/Y2022/V42/I3/92

Zhou, Z.H. (2016), *Machine Learning*, Tsinghua University Press, Beijing, BJ, China.